Am J Cancer Res 2022;12(8):3662-3678
www.ajcr.us /ISSN:2156-6976/ajcr0143892

Original Article

COA3 overexpression promotes non-small cell lung cancer metastasis by reprogramming glucose metabolism

Hongwei Lin[1*], Yanjun Gao[1*], Kang Sun[2], Qian Zhang[1], Yujuan Li[1], Min Chen[1], Faguang Jin[1]

[1]Department of Respiratory and Critical Care Medicine, Tangdu Hospital, The Air Force Medical University, Xi'an 710038, Shaanxi Province, China; [2]Department of Respiratory and Critical Care Medicine, The 989th Hospital of Joint Logistics Support Force of Chinese People's Liberation Army, Luoyang 471000, Henan Province, China. [*]Equal contributors.

Received May 3, 2022; Accepted July 11, 2022; Epub August 15, 2022; Published August 30, 2022

Abstract: Recent advances in cancer research have revealed a close relationship between mitochondrial dysfunction and cancer development. Human COX assembly factor 3 (COA3), also known as CCDC56, is a mitochondrial transmembrane protein responsible for cytochrome c oxidase (COX) protein complex assembly. However, the clinical implication and biological functions of COA3 remain unexplored in human cancers, including non-small cell lung cancer (NSCLC). Here, we found that COA3 is overexpressed at both mRNA and protein levels in human NSCLC cells, mainly as a result of decreased miR-338-3p level. The protein expression level of COA3 is positively associated with lymph node metastasis and predicts poor survival in patients with NSCLC. Silencing of COA3 significantly attenuated, while forced COA3 expression enhanced the migration and invasiveness of NSCLC cells. Mechanistically, we found that aerobic glycolysis, induced at least in part by dynamic-related protein 1 (DRP1) phosphorylation-mediated mitochondrial fragmentation, contributed to COA3-promoted NSCLC metastasis. Together, our study illustrates that COA3 plays a crucial role in NSCLC carcinogenesis, implying COA3 as a prognostic marker and treatment target in NSCLC.

Keywords: COA3, metastasis, mitochondrial fragmentation, glycolysis, NSCLC

Introduction

Non-small cell lung cancer (NSCLC) is one of the most common causes of cancer-related deaths worldwide [1]. Despite significant advances in the management of NSCLC, the survival of NSCLC patients remains poor for our incomplete understanding of the molecular mechanisms driving this malignancy [2, 3]. Therefore, it is necessary to study key factors associated with the progression of NSCLC to develop novel therapies for treatment of this malignancy.

In addition to their roles in energy production, mitochondria also play crucial roles in the regulations of cell death and redox homeostasis [4]. The functions of mitochondria are closely associated with their morphology, which is dynamically regulated by fission and fusion events [5]. Mitochondrial dynamic dysfunction has been reported to play crucial roles in the development of many human diseases, including cancer [6]. In addition, several lines of evidence also suggested that mitochondrial dynamic dysfunction is a common cause of reprogrammed metabolism in cancer cells [6, 7]. Human cytochrome c oxidase (COX) assembly factor 3 (COA3), also known as CCDC56, is a mitochondrial transmembrane protein involved in the assembly of COX protein complex [8, 9]. However, the clinical implication and biological functions of COA3 remain unexplored in human cancers, especially in metabolism reprogramming.

In the present study, we systematically analyzed the expression profile, clinical implication and functions of COA3 in NSCLC.

Materials and methods

Cell lines

Human NSCLC cell lines (A549, H1299, HCC-827, H1975, H460 and H1650) and bronchial epithelial cell line (BEAS-2B) were derived from

the American Type Culture Collection (ATCC). These cell lines were cultured in RPMI-1640 medium (Gibco) containing 10% fetal bovine serum (FBS) with 5% CO_2 at 37°C. All cell lines were mycoplasma-free and tested by short tandem repeat (STR) analysis.

Knockdown or over-expression of target genes

Synthesized siRNA duplexes targeting COA3 (si-COA3) and non-targeting control siRNA (siCtrl) were prepared by chemical synthesis in GeneChem, China. The target sequence of si-COA3 was 5'-GAAGCUGACACCCGAGCAA-3' (siCOA3#1) and 5'-GGUUACACCUUCUACUCGA-3' (siCOA3#2). For overexpression of COA3, the coding sequence of COA3 was amplified by PCR assay and then inserted into pcDNA™3.1 vector. Transfections of siRNAs or expression vectors were performed with Lipofectamine 3000 (Invitrogen, USA).

Western blotting assay

Cell lysates were heated in boiling water and then separated by sodium dodecyl sulfate-polyacrylamide gel electrophoresis (SDS-PAGE). Protein was transferred onto PVDF membrane and probed with primary antibodies against COA3 (Abcam, ab122199), ZO-1 (Proteintech, 20742-1-AP), E-cadherin (Proteintech, 20874-1-AP), Vimentin (Proteintech, 10366-1-AP), N-cadherin (Proteintech, 22018-1-AP), MFN1 (Proteintech, 13798-1-AP), MFN2 (Proteintech, 12186-1-AP), OPA1 (Proteintech, 27733-1-AP), DRP1 (Proteintech, 12957-1-AP), DRP1-S616 (Cell Signaling, #3455), DRP1-S637 (Abcam, ab193216), Fis1 (Proteintech, 10956-1-AP), MFF (Proteintech, 17090-1-AP) and β-actin (Proteintech, 66009-1-Ig).

Quantitative real-time PCR (qRT-PCR) assay

Extracted RNA was reversely-transcribed with a PrimeScript® RT reagent kit (Takara, Japan). PCR amplification was performed using the qPCR SYBR Green Master Mix (Takara Biotechnology). Primers used were provided in Table S1. Relative mRNA expression level was normalized to β-actin.

Cell proliferation and colony formation assays

For cell proliferation, 2000 NSCLC cells were plated in 96-well plates. An MTS assay kit (Abcam, ab197010) was used to measure cell viability at the indicated time points following the manufacturer's instruction. For colony formation, cells were plated at a concentration of 1000 cells per well in 6-well plates and cultured for 12 days. Colonies were stained with crystal violet and counted.

Cell migration and invasion assays

To determine cell migration ability, a scratch was made with a yellow plastic pipette in 6-plate well when cells grown to about 85% confluency. Forty-eight hours after seeding, cell migration was photographed. To determine cell invasion ability, transwell filter chambers purchased from Corning Biosciences in 24-well dishes were used. Forty-eight hours after seeding, invaded cells were fixed, stained and counted.

Tissue collection and immunohistochemistry (IHC) analysis

A total of 311 pairs tumor and non-tumor tissues of NSCLC were used in this study. Among them, 30 pairs used for qRT-PCR analysis were collected at the Institute of Pulmonary Diseases of the Air Force Medical University between 2019 and 2020. The other 281 pairs used for IHC analysis were purchased from Shanghai Outdo Biotech (Shanghai, China), which was collected between 2011 and 2015 with a median duration of follow-up of 42 months (2 to 120 months). The research protocols were approved by the ethics committee of the Air Force Medical University in Xi'an, China. Informed consent was obtained from all the patients in the study.

IHC staining of target proteins was performed as follows: Tissue sections were rehydrated, antigen retrieved, and blocked with 5% BSA. Slides were then incubated with primary antibodies targeting COA3 (Proteintech, 20427-1-AP, 1:250 dilution) or Ki-67 (Proteintech, 27309-1-AP, 1:250 dilution) at 4°C overnight. The signals were detected using an IHC detection kit (MXB, Fuzhou, China).

Cell cycle and apoptosis assays

NSCLC cells were collected and resuspended in cold phosphate-buffered saline (PBS). Cell cycle was analyzed using a cell cycle detection kit (ab112116, Abcam). Briefly, cells were washed three times in cold PBS and fixed in cold 70% ethanol for 10 h. After that, cells were

incubated in 1 mL staining solution containing RNase and propidium iodide (PI) for 30 min in the dark at 4°C. The results were finally evaluated by Flow cytometry (Beckman, Fullerton, CA). In addition, a cell apoptosis detection kit (F-6012, US Everbright Inc) was used for cell apoptosis analysis. Briefly, NSCLC cells were incubated in 0.5 mL binding buffer, 5 μL Annexin 5-FITC and PI for 25 min in the dark at room temperature. The results were finally evaluated by Flow cytometry (Beckman, Fullerton, CA).

In vivo metastasis assay

The tail vein metastatic nude mice model was used to determine *in vivo* metastasis ability of NSCLC cells. Briefly, a total of 2×10^6 H1299 cells with COA3 knockdown or HCC827 cells with COA3 overexpression were injected into the tail vein of 4-6-week-old male BALB/c nude mice. The mice were housed in SPF environment at temperature 22-25°C on a 12 h light/dark cycle with free access to water and standard food. Mice were euthanized five weeks after cells injection and their lungs were dissected, fixed in formalin, embedded in paraffin and histologically analyzed by H&E staining assay. For H&E staining, sections were dewaxed and rehydrated. After that, sections were stained with hematoxylin for 10 s and blued for 3 min in water. Next, sections were counter stained with eosin solution for 30 s and washed in water. The staining images were acquired using a microscope (Olympus).

Animal experiments were approved by the Institutional Animal Care and Use Committee of the Air Force Medical University.

Mitochondria staining

Mitotracker Green FM (M7514, Invitrogen, USA), a green fluorescent dye, was used for mitochondrial morphology analysis. Briefly, NSCLC cells were seeded in confocal dish and incubated with Mito Tracker green FM for 25 min. Images were acquired using an confocal microscope (Olympus).

Oxygen consumption rate (OCR) measurement

Seahorse XF24 analyzer (Boston, USA) was used for evaluation of OCR in NSCLC cells. Cells (8×10^3) were seeded into an XF24-well cell culture plate. Before OCR detection, Seahorse XF basal media was used for equilibration. Measurements were conducted following the manufacturer's instructions. Finally, the OCR was normalized to total protein content.

Measurement of mitochondrial respiratory chain complexes activities

To measure the activities of mitochondrial respiratory chain complexes I-V, a commercial complete oxidative phosphorylation (OXPHOS) activity assay kit derived from Abcam (ab-110419) was used. Detections were performed according to the manufacturer's protocols. Absorption values were measured using a Bio-Rad microplate reader. Finally, the activities were normalized to total protein content.

Measurement of glucose consumption, lactate production and PH value

For measurement of glucose consumption and lactate production, the changes of glucose or lactate concentration after 24 h cell culture were determined. Detection was conducted using a glucose or lactate detection kit (Nanjing jiancheng Bioengineering institute, China) following the manufacturer's protocol. For measurement of PH value, a calibrated PB-11 Basic pH Meter was used. The device was calibrated with three calibration solutions before the measurement. Calibration and measurement were performed following the manufacturer's instruction at 37°C.

Metabolite measurements

NSCLC cells were washed three times with a mannitol solution. Then, metabolites extraction was performed. Briefly, cells were suspended in PBS and frozen in liquid nitrogen. After that, cells were resuspended in 500 μL of methanol aqueous solution (80%), followed by centrifugation at 4°C for 30 min (13,000 g). Metabolites in the supernatant were lyophilized for metabolomics analysis with gas chromatography-mass spectrometry (GC-MS) following the manufacturer's protocol. Finally, metabolomics were normalized to total protein content.

Statistical analysis

Statistical analysis was conducted with SPSS software (17.0 version). The data was presented as mean ± standard error of the mean (SEM), and $P<0.05$ was considered statistically

significant. The results were analyzed by two-tailed Student's t-test (between two groups) or one-way analysis of variance (ANOVA) with Tukey's post-hoc test (more than two groups). For survival analysis of NSCLC patients with different COA3 expression levels, the Kaplan-Meier method and log-rank test were used.

Results

Upregulation of COA3 predicts poor survival for NSCLC patients

We first analyzed the expression of COX assembly factor 3 (COA3) in The Cancer Genome Atlas Program (TCGA) dataset with the online web portal UALCAN [10]. Both mRNA and protein expressions of COA3 were significantly upregulated in non-small cell lung cancer (NSCLC) tissues as compared to normal lung tissues (**Figure 1A**). To confirm the expression pattern of COA3 in NSCLC, we assessed COA3 expression in 30 pairs NSCLC and surrounding non-tumorous tissues at mRNA level using quantitative reverse transcription PCR (qRT-PCR) assay. The mRNA expression levels of COA3 were significantly upregulated in NSCLC tissues as compared to paired normal lung tissues (**Figure 1B**). Consistently, IHC staining of COA3 at the protein level in another cohort of 281 pairs NSCLC and adjacent non-tumor tissues also revealed that COA3 expression was markedly higher in NSCLC tissues than in adjacent non-tumor tissues (**Figure 1C**). Additionally, up-regulation of COA3 was also found in a panel of human NSCLC cell lines, showing that COA3 expressions at both mRNA and protein levels were obviously higher in NSCLC cell lines than in an immortalized bronchial epithelial cell line (**Figure 1D**, **1E**). To reveal the clinical relevance of COA3 expression in NSCLC, the correlation between the protein expression levels of COA3 and the survival of patients were analyzed. COA3 expression at protein level was inversely correlated with overall survival (OS) of NSCLC patients (**Figure 1F**). In addition, COA3 expression at protein level was also positively associated with the metastatic status of NSCLC patients ($P<0.012$) (Table S2). Together, these data demonstrate that COA3 are significantly upregulated in NSCLC, which predicts poor survival for NSCLC patients.

Silencing of COA3 suppressed NSCLC cell migration and invasion by inhibiting epithelial-mesenchymal transition (EMT)

To explore the role of COA3 in tumorigenesis of NSCLC, we silenced COA3 expression in two NSCLC cell lines (H1299 and H1975 cells) expressing relatively high COA3 (indicated in **Figure 1D**, **1E**). Successful silencing of COA3 expression in H1299 and H1975 cells was confirmed by qRT-PCR and western blotting assays (**Figure 2A**, **2B**). Silencing of COA3 resulted in a significant reduction in cell migration and invasion (**Figure 2C**, **2D**), but had no effect on proliferation and colony-forming abilities of NSCLC cells (Figure S1A, S1B). We next explored whether COA3 induced epithelial-mesenchymal transition (EMT), which is a prerequisite mechanism in tumor metastasis. COA3 silencing increased epithelial markers of ZO-1 and E-cadherin, while decreased mesenchymal markers of N-cadherin and vimentin (**Figure 2E**, **2F**), suggesting that COA3 silencing may suppress metastasis of NSCLC by inhibiting the EMT program.

To further study the role of COA3 in NSCLC metastasis *in vivo*, stable COA3 knockdown (shCOA3) or control (shCtrl) H1299 cells (Figure S1C and S1D) were injected into the nude mice through the tail vein. Five weeks after cells injection, metastasis in the lungs was examined by hematoxylin and eosin (H&E) staining. We found a significant decrease of microscopically visible metastatic tumor nodules in COA3 knockdown group as compared with the control group (**Figure 2G**).

Forced COA3 expression promoted NSCLC metastasis

To further validate the function of COA3 in NSCLC metastasis, COA3 was upregulated in HCC827 and H460 cells expressing low levels of COA3 (indicated in **Figure 1D**, **1E**). Successful overexpression of COA3 was confirmed by qRT-PCR and western blotting assays (**Figure 3A**, **3B**). Our results showed that forced COA3 expression markedly enhanced the migration and invasion capacities of HCC827 and H460 cells (**Figure 3C**, **3D**). Additionally, a significant increase in microscopically visible metastatic nodules was observed in the lungs of nude

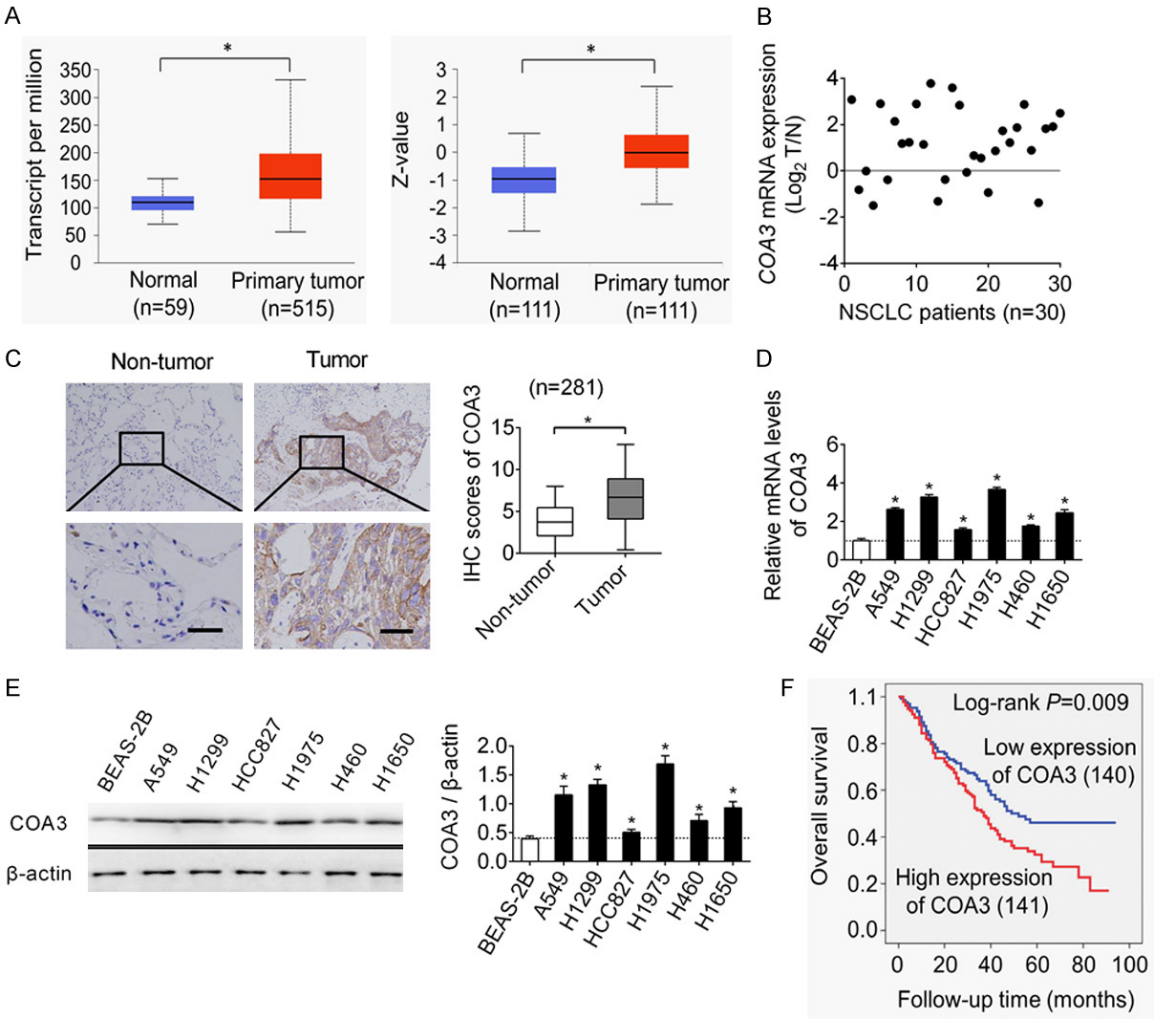

Figure 1. Upregulation of COA3 predicts poor survival for NSCLC patients. A. The expressions of COX assembly factor 3 (COA3) were analyzed in non-small cell lung cancer (NSCLC) of The Cancer Genome Atlas Program (TCGA) dataset at both mRNA (Left panel) and protein (Right panel) levels. B. Quantitative reverse transcription PCR (qRT-PCR) analysis for mRNA expression levels of COA3 in 30 pairs NSCLC and surrounding non-tumorous tissues. C. The protein expression levels of COA3 were determined by IHC staining analysis in another cohort of 281 pairs NSCLC and adjacent non-tumor tissues. D and E. COA3 expression at both mRNA and protein levels were determined in a panel of human NSCLC cell lines by qRT-PCR and western blotting assays. F. Correlation between the protein expression levels of COA3 and survival of NSCLC patients was analyzed.

mice from COA3 overexpression (COA3) group than those from control (empty vector, EV) group (**Figure 3E**). Overall, these data indicate that forced COA3 expression promotes NSCLC metastasis.

COA3 up-regulation is mainly caused by decreased miR-338-3p expression in NSCLC

Previous studies have demonstrated that decreased microRNA (miRNA) is a common means of upregulating oncogenes during tumorigenesis. To determine whether COA3 upregulation in NSCLC is mediated by decreased miRNA level, we screened potential miRNAs targeting COA3 using the microRNA Data Integration Portal (mirDIP) [11]. We found that, among the top five screened miRNAs (Figure S2A), only miR-338-3p transfection decreased COA3 expression at both mRNA and protein levels in H1299 and H1975 cells (**Figure 4A**, **4B**). Additionally, COA3 expression was negatively associated with miR-338-3p level in tumor tissues from 30 NSCLC patients (**Figure 4C**). Meanwhile, decreased miR-338-3p levels were also observed in tumor tissues of NSCLC as

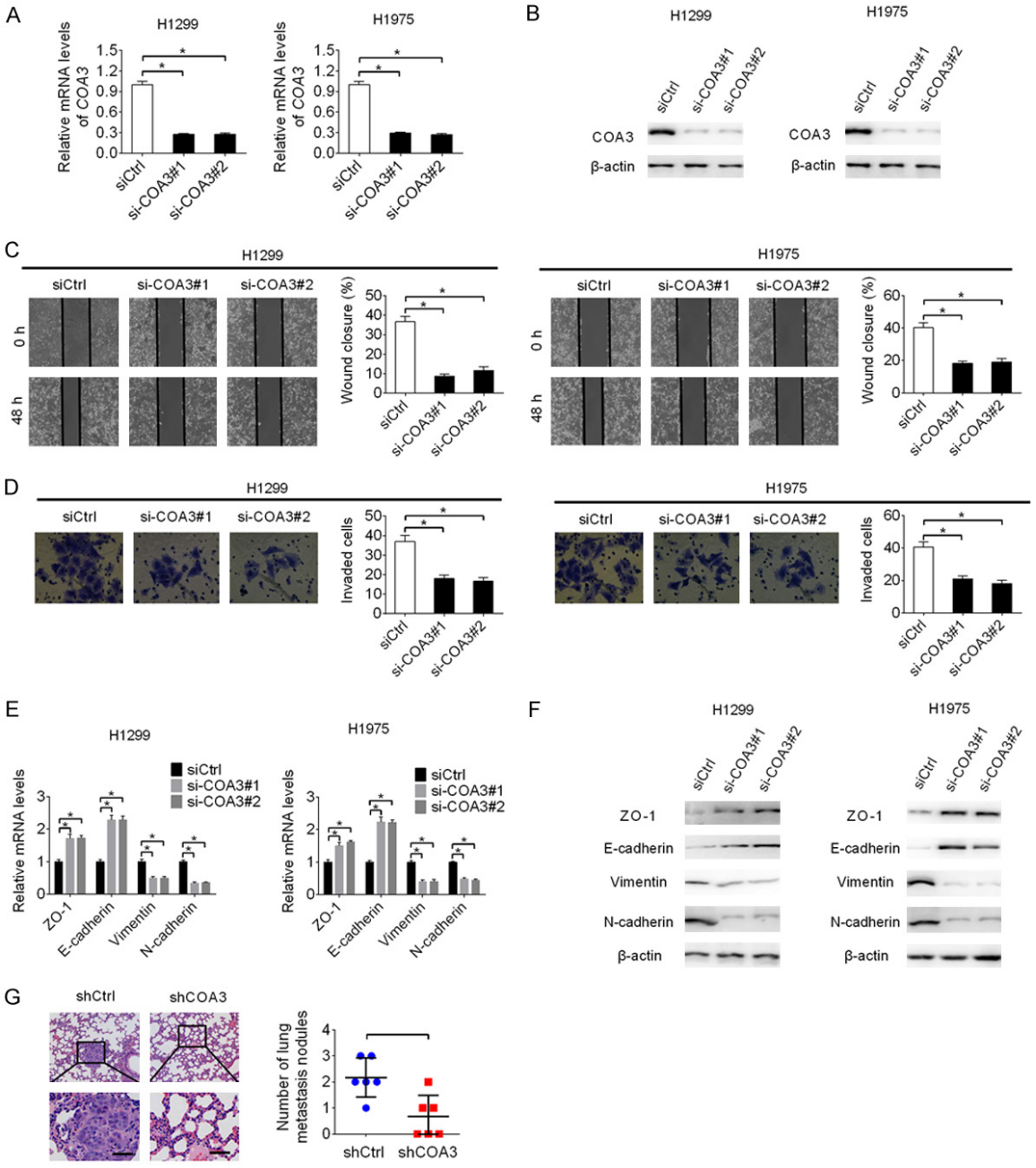

Figure 2. Silencing of COA3 suppressed NSCLC cell migration and invasion by inhibiting epithelial-mesenchymal transition (EMT). A and B. qRT-PCR and Western blotting assays were conducted for COA3 expression in H1299 and H1975 cells with COA3 knockdown. C and D. The effects of COA3 knockdown on cell migration and invasion were evaluated in H1299 and H1975 cells. E and F. The expressions of EMT markers were detected in H1299 and H1975 cells. G. Hematoxylin and eosin (H&E) staining for metastatic nodules in the lungs of nude mice injected with COA3 knockdown (shCOA3) or control (shCtrl) H1299 cells.

compared with corresponding non-tumor tissues (n = 30) (**Figure 4D**). In keeping with this, bioinformatics analysis in TCGA data using UALCAN also revealed a significant decrease of miR-338 level in NSCLC as compared with normal lung tissues (Figure S2B). Nevertheless, no survival difference existed between miR-338 high and low NSCLC patients (Figure S2B). Moreover, luciferase reporter assay was used to explore whether miR-338-3p binds to the 3'-UTR of COA3 in NSCLC cells (**Figure 4E**). We found that miR-338-3p transfection obviously

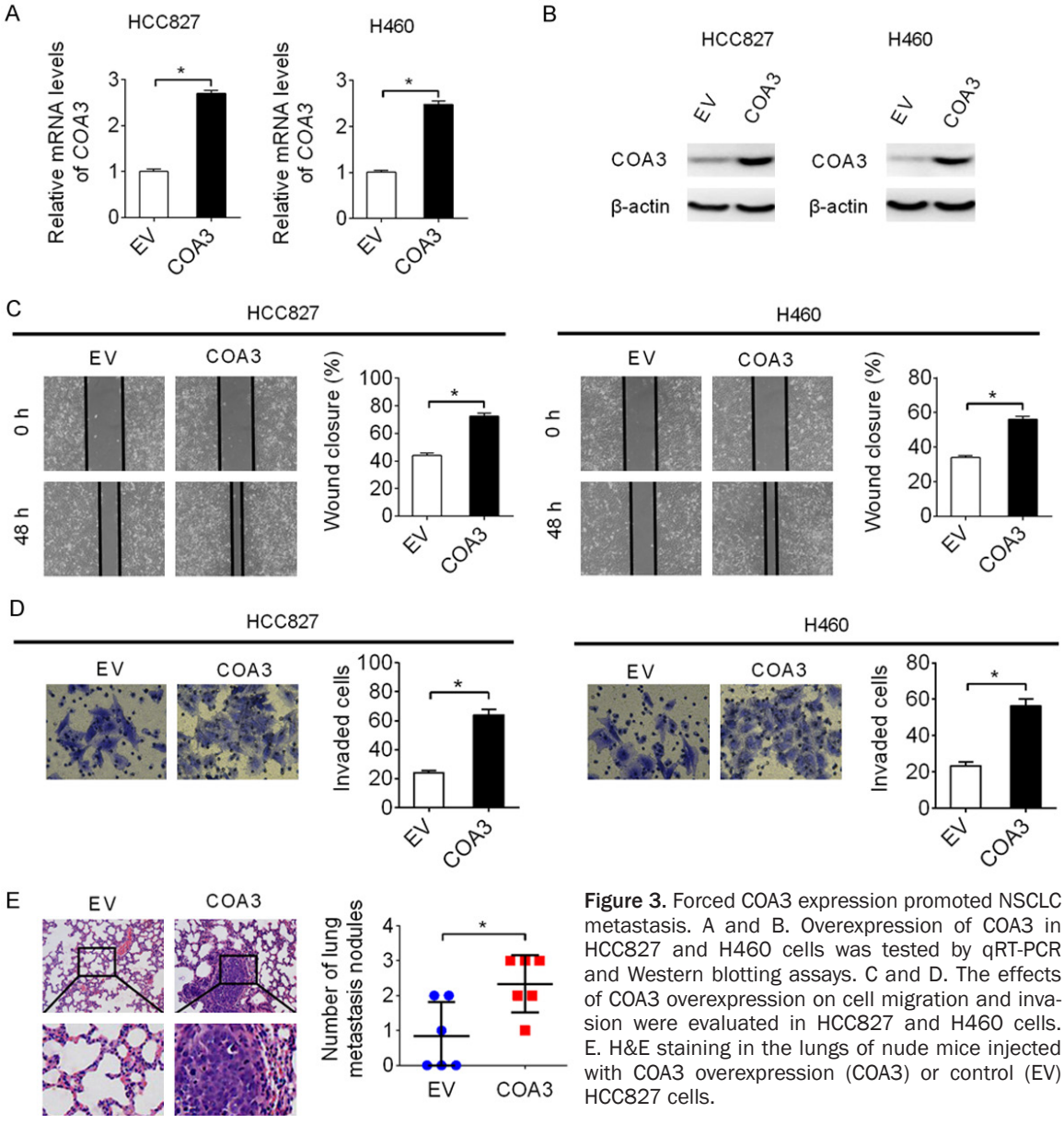

Figure 3. Forced COA3 expression promoted NSCLC metastasis. A and B. Overexpression of COA3 in HCC827 and H460 cells was tested by qRT-PCR and Western blotting assays. C and D. The effects of COA3 overexpression on cell migration and invasion were evaluated in HCC827 and H460 cells. E. H&E staining in the lungs of nude mice injected with COA3 overexpression (COA3) or control (EV) HCC827 cells.

decreased the luciferase activity of wild-type but not mutant construct of 3'-UTR of COA3 in NSCLC cells (**Figure 4F**). Moreover, miR-338-3p transfection significantly attenuated the promoting effect of COA3 on NSCLC metastasis (**Figure 4G-I**).

COA3 promotes mitochondrial fragmentation in NSCLC cells by phosphorylating Ser616 of DRP1

Increased mitochondrial fragmentation plays crucial roles in the progression of various human cancers [12]. Given that COA3 was reported to promote mitochondrial fragmentation in HeLa cells [13], we thus explored the underlying mechanism of COA3-promoted metastasis by evaluating the effect of COA3 on mitochondria fragmentation in NSCLC cells. As shown in **Figure 5A**, mitochondria were significantly elongated upon COA3 knockdown in H1299 cells, while fragmented upon COA3 overexpression in HCC827 cells.

To gain insight into the molecular basis of COA3-induced mitochondrial fragmentation in NSCLC cells, the effects of COA3 on the expressions of mitochondrial fission and fusion

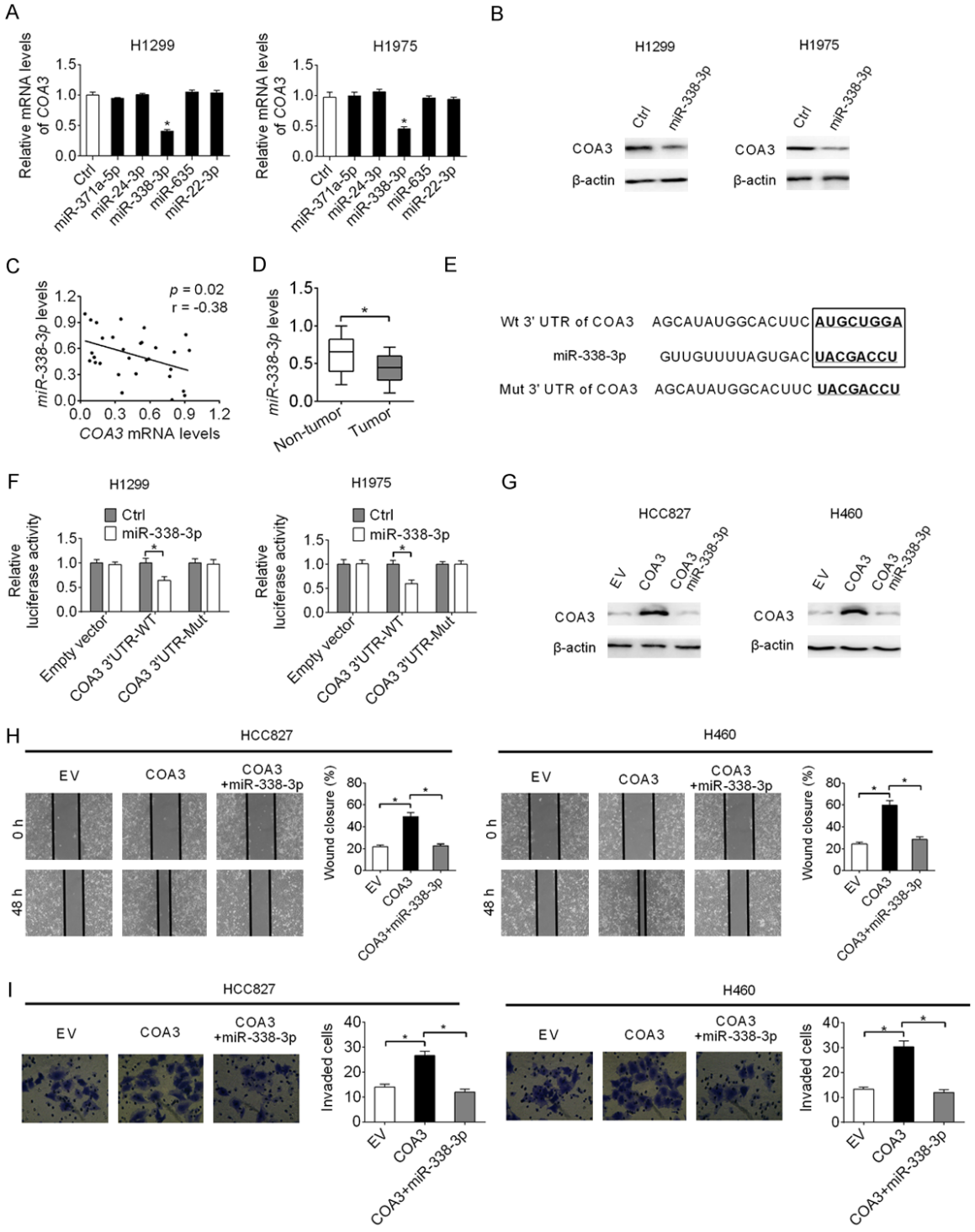

Figure 4. COA3 up-regulation is mainly caused by decreased miR-338-3p expression in NSCLC. A and B. Expressions of COA3 were detected by qRT-PCR and Western blotting assays in H1299 and H1975 cells transfected with different microRNAs (miRNAs). C. Correlation between the expression levels of miR-338-3p and COA3 was analyzed in tumor tissues from 30 NSCLC patients. D. The expression levels of miR-338-3p were determined in 30 paired tumor and surrounding non-tumorous tissues. E. The wild-type or mutant sequences of COA3 3'-UTR. F. The luciferase activity of the wild-type or mutant COA3 3'-UTR co-transfected with miR-338-3p was measured. G. The expression levels of COA3 were detected by western blotting assay in HCC827 and H460 cells with indicated treatment. H and I. Cell migration and invasion were analyzed in HCC827 and H460 cells with indicated treatment.

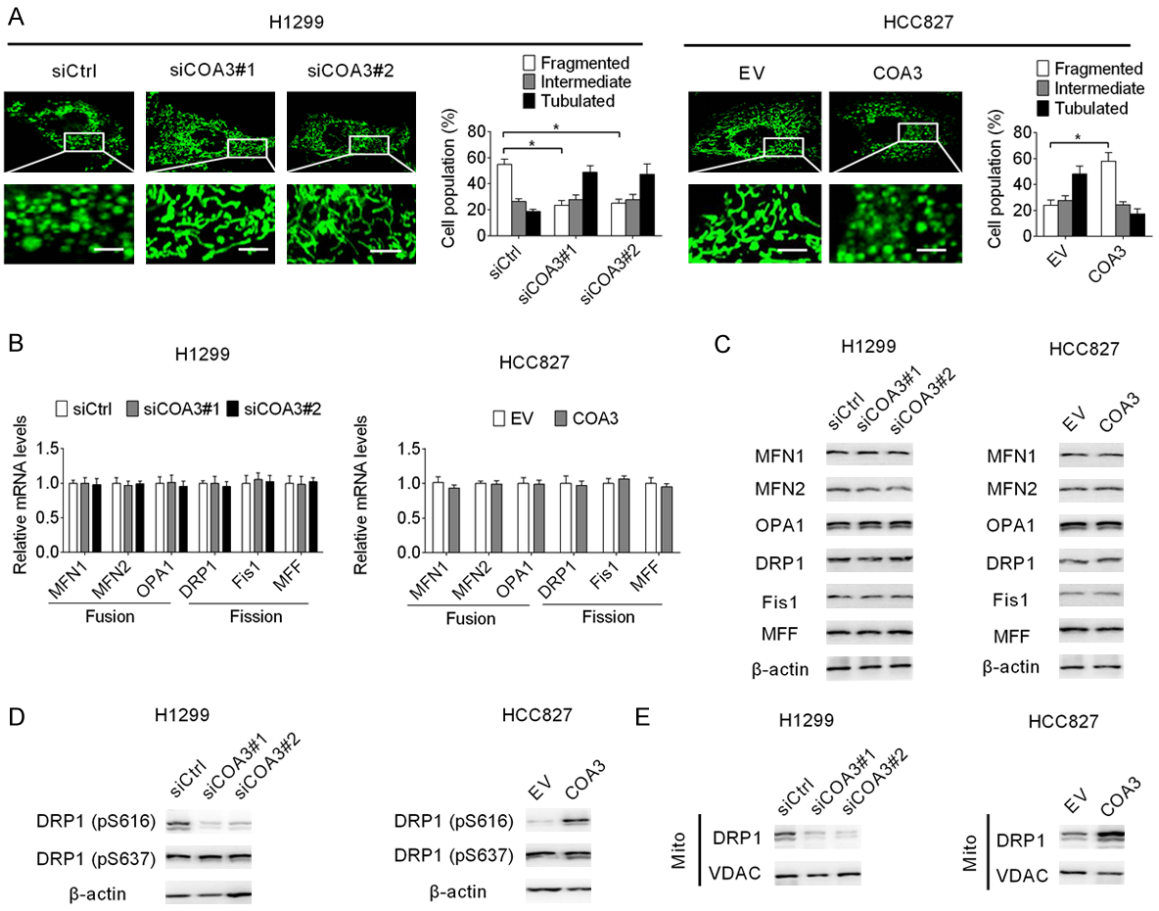

Figure 5. COA3 promotes mitochondrial fragmentation in NSCLC cells by phosphorylating Ser616 of DRP1. A. Mitochondrial morphology was assessed by staining with green fluorescent reporter targeting mitochondria in H1299 and HCC827 cells with COA3 knockdown or overexpression. Scale bar, 1 μm. B and C. The expressions of mitochondria dynamic regulators mitofusin 1 (MFN1), mitofusin 2 (MFN2), Optic Atrophy 1 (OPA1), dynamin-related protein1 (DRP1), fission 1 (FIS1) and mitochondrial fission factor (MFF) were detected by qRT-PCR and Western blotting assays in H1299 and HCC827 cells with COA3 knockdown or overexpression. D. DRP1 phosphorylation at Ser616 and Ser637 was evaluated in in H1299 and HCC827 cells. E. DRP1 expression in cytoplasm or mitochondria was analyzed in H1299 and HCC827 cells.

regulators were evaluated. Unexpectedly, on obvious changes in the expressions of mitofusin 1 (MFN1), mitofusin 2 (MFN2), Optic Atrophy 1 (OPA1), dynamin-related protein1 (DRP1), fission 1 (FIS1) and mitochondrial fission factor (MFF) were observed upon COA3 knockdown or overexpression (**Figure 5B**, **5C**). Given that phosphorylation is a major mechanism controlling the function of DRP1, the core components of the mitochondrial fission machinery, we determined the potential contribution of DRP1 phosphorylation in COA3-induced mitochondrial fragmentation. Knockdown of COA3 significantly decreased the phosphorylation of DRP1 at Ser616, but had no obvious influence on phosphorylation at Ser637. In contrast, forced expression of COA3 markedly increased DRP1 phosphorylation at Ser616 (**Figure 5D**). It has been demonstrated that DRP1 phosphorylation at Ser616 stimulated mitochondrial fission by recruiting DRP1 to mitochondria [14]. Therefore, we investigated whether COA3 promote the translocation of DRP1 from cytoplasm to mitochondria. Knockdown of COA3 markedly decreased mitochondria-localized DRP1, while overexpression of COA3 increased mitochondria-localized DRP1 (**Figure 5E**). Together, these data indicate that COA3 promotes mitochondrial fragmentation in NSCLC cells by phosphorylating Ser616 of DRP1.

COA3 enhances aerobic glycolysis in NSCLC cells

Mitochondria play a central role in metabolism regulation. Given that COA3 promotes mitochondrial fragmentation in NSCLC cells, we next explored whether COA3 participates in mitochondrial metabolism reprogramming in NSCLC cells. Accordingly, the effects of COA3 on oxygen consumption rate (OCR), activities of oxidative phosphorylation (OXPHOS) complexes, and cellular ATP levels were measured in NSCLC cells. We found that knockdown of COA3 resulted in increased OCR, activities of OXPHOS complexes (I, II, III and V) and ATP levels in H1299 cells, whereas overexpression of COA3 suppressed these mitochondrial metabolic phenotypes in HCC827 cells (**Figure 6A-C**). In light of the tight association between mitochondrial metabolism and aerobic glycolysis [15], we explored the role of COA3 in aerobic glycolysis in NSCLC cells. As shown in **Figure 6D-F**, COA3 silencing decreased glucose uptake and lactate production, while increased PH value of cell culture medium of H1299 cells. Conversely, forced expression of COA3 exhibited the opposite effects on these glycolytic phenotypes in HCC827 cells. Consistently, metabolites analysis revealed that COA3 knockdown significantly decreased the intracellular levels of glycolytic intermediates, while increased tricarboxylic acid (TCA) cycle intermediates in H1299 cells. By contrast, forced expression of COA3 exhibited the opposite effects in HCC827 cells (**Figure 6G**). Collectively, these data suggest that COA3 enhances aerobic glycolysis in NSCLC cells.

COA3 enhances aerobic glycolysis of NSCLC cells, at least in part, by promoting mitochondrial fragmentation

We next assessed whether COA3 enhances aerobic glycolysis by promoting mitochondrial fragmentation in NSCLC. The results showed increased mitochondrial fragmentation by COA3 overexpression was dramatically reversed upon suppression of mitochondrial fragmentation by mitochondrial division inhibitor 1 (Mdivi-1, a specific inhibitor of DRP1) treatment in HCC827 and H460 cells. Meanwhile, we found that suppression of mitochondrial fragmentation also reversed COA3 overexpression-induced glucose metabolism reprogramming from mitochondrial OXPHOS to aerobic glycolysis (**Figure 7B-H**). These data indicate that COA3 overexpression enhances aerobic glycolysis in NSCLC cells, at least in part, by promoting mitochondrial fragmentation.

COA3 promotes NSCLC metastasis mainly through enhancing mitochondrial fragmentation-induced aerobic glycolysis

Aerobic glycolysis has been reported to play a crucial role in metastasis of human cancers [16]. To verify whether COA3 promotes NSCLC metastasis by activating mitochondrial fragmentation-induced aerobic glycolysis, the restoring effects of mitochondrial fragmentation-induced aerobic glycolysis on NSCLC-promoted migration and invasion of NSCLC cells were evaluated. The results showed that suppression of mitochondrial fragmentation by Mdivi-1 significantly attenuated COA3 overexpression-promoted migration and invasion of NSCLC cells (**Figure 8A**, **8B**). Similar results were also observed when glycolysis was suppressed by galactose (**Figure 8C**, **8D**). These data suggest that COA3 functions as a potential oncogene in NSCLC metastasis by enhancing mitochondrial fragmentation-induced aerobic glycolysis.

Discussion

Human cytochrome c oxidase (COX) assembly factor 3 (COA3), also known as CCDC56, is a mitochondrial transmembrane protein participates in the assembly of COX protein complex [8, 9]. However, the clinical implication and biological functions of COA3 remain largely unknown in human cancers. In the present study, we revealed that COA3 was upregulated in NSCLC and its upregulation predicted worse survival in patients with NSCLC. Consistently, COA3 expression was also positively correlated with metastasis in lymph node. These results suggested that COA3 might be a promising prognostic marker for NSCLC.

Upregulation of COA3 and its positive relationship with lymph node metastasis implies that COA3 may play a role in NSCLC carcinogenesis. We demonstrated that knockdown of COA3 significantly impaired the motility and invasiveness of NSCLC cells, while had no significant effect on proliferation and colony-forming abili-

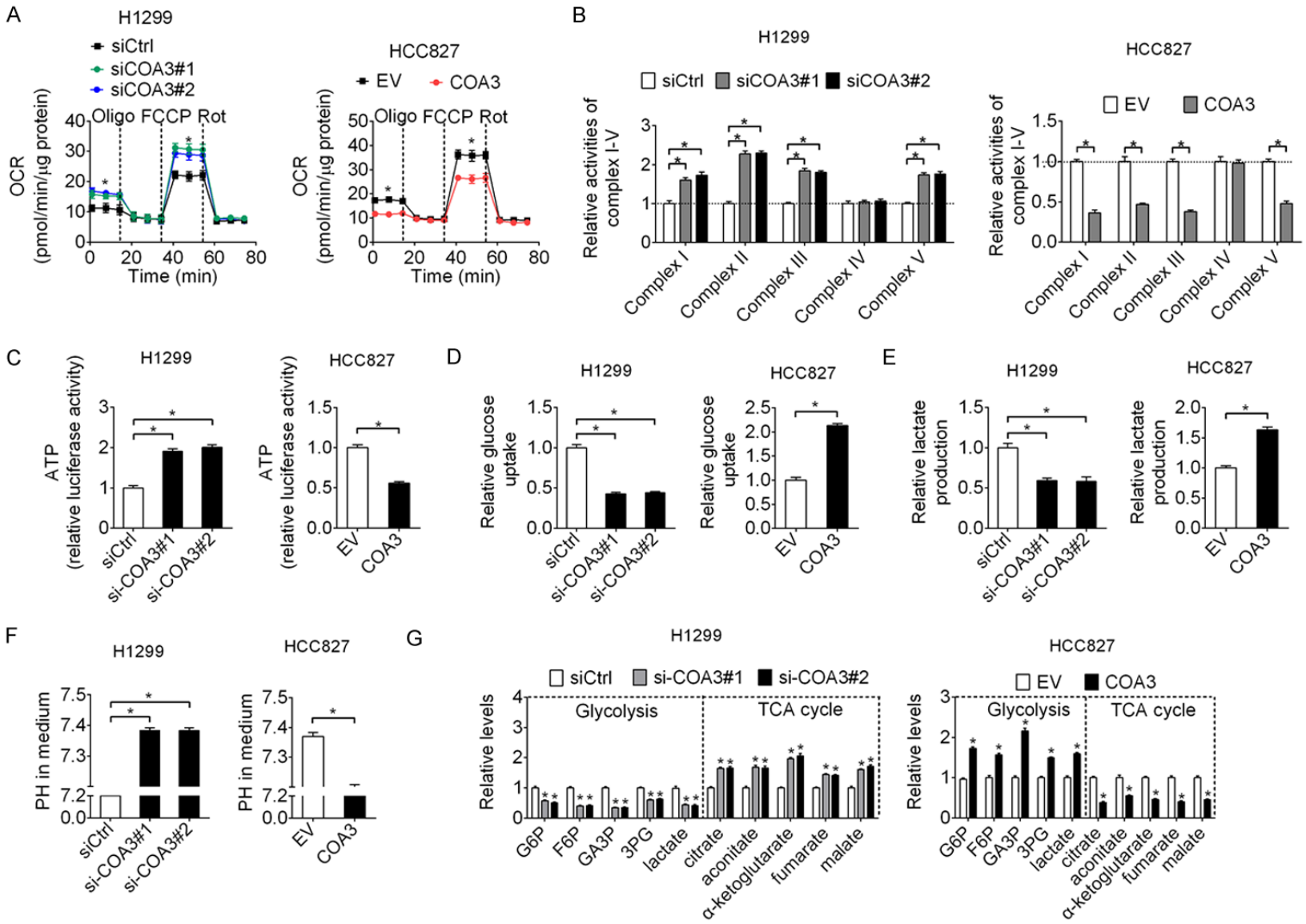

Figure 6. COA3 enhances aerobic glycolysis in NSCLC cells. (A) Oxygen consumption rate (OCR) was measured in NSCLC cells with COA3 knockdown or overexpression. (B) The activities of oxidative phosphorylation (OXPHOS) complexes were determined in NSCLC cells with COA3 knockdown or overexpression. (C) The production of ATP was determined in NSCLC cells with COA3 knockdown or overexpression. (D-F) Glucose uptake (D), lactate production (E) and PH value in cell culture medium (F) were measured in NSCLC cells. (G) Glycolytic and tricarboxylic acid (TCA) cycle intermediates were detected in NSCLC cells.

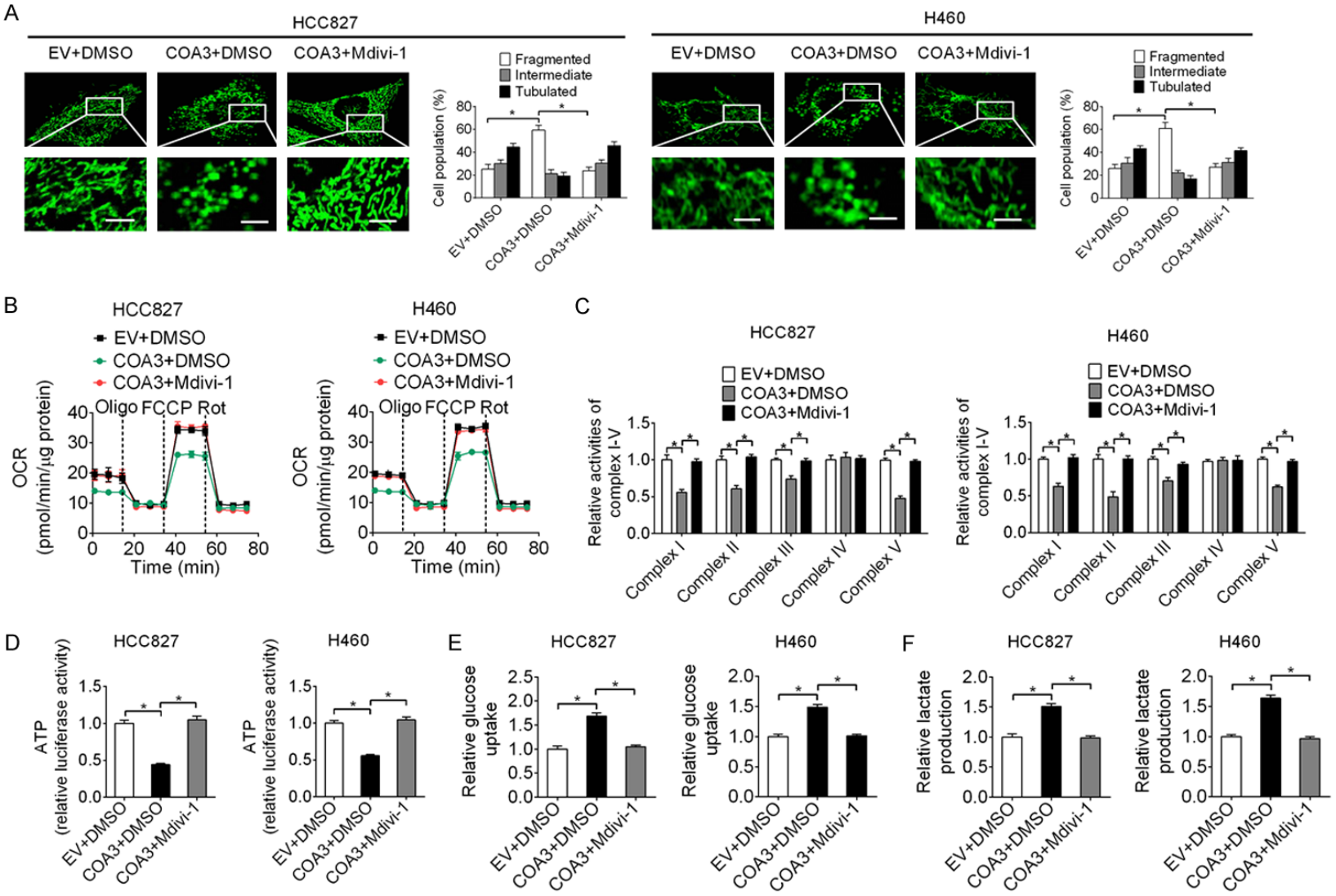
A
HCC827
EV+DMSO
COA3+DMSO
COA3+Mdivi-1
Fragmented
Intermediate
Tubulated
Cell population (%)
H460
B
HCC827
H460
EV+DMSO
COA3+DMSO
COA3+Mdivi-1
Oligo FCCP Rot
OCR (pmol/min/μg protein)
Time (min)
C
HCC827
H460
Relative activities of complex I-V
Complex I
Complex II
Complex III
Complex IV
Complex V
D
ATP (relative luciferase activity)
E
Relative glucose uptake
F
Relative lactate production

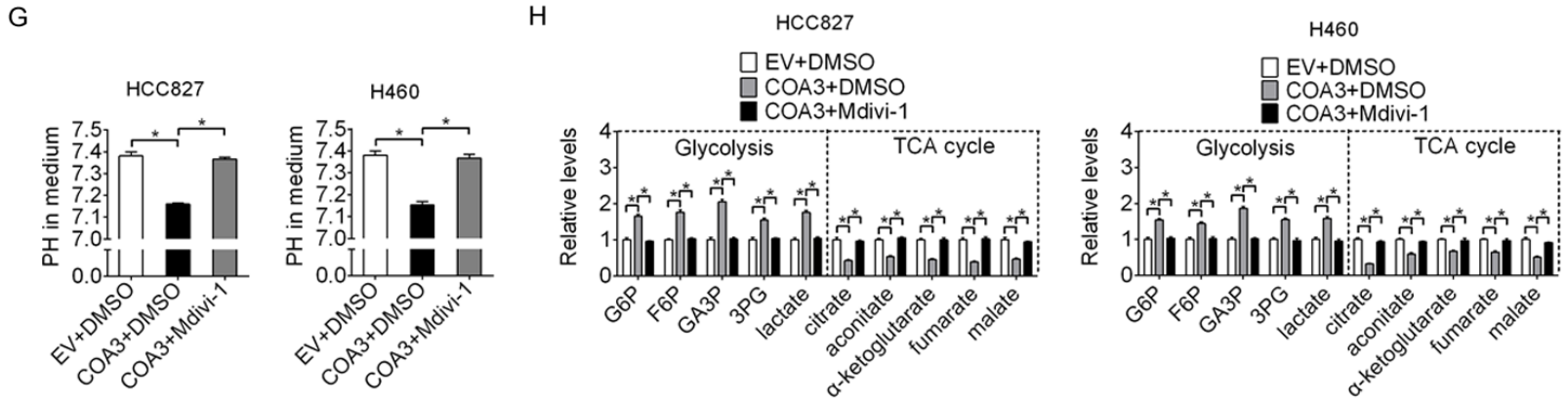

Figure 7. COA3 enhances aerobic glycolysis of NSCLC cells, at least in part, by promoting mitochondrial fragmentation. (A) Mitochondrial morphology was assessed by staining with green fluorescent reporter targeting mitochondria in HCC827 and H460 cells with treatment as indicated. Scale bar, 1 μm. (B-D) The oxygen consumption rate (B) activities of oxidative phosphorylation (C) and production of ATP (D) were determined in HCC827 and H460 cells with treatment as indicated. (E-G) Measurements of glycolytic phenotypes, including glucose consumption (E), lactate production (F) and PH-value in cell culture medium (G) in HCC827 and H460 cells with treatment as indicated. (H) Glycolytic and TCA cycle intermediates were measured in HCC827 and H460 cells with treatment as indicated.

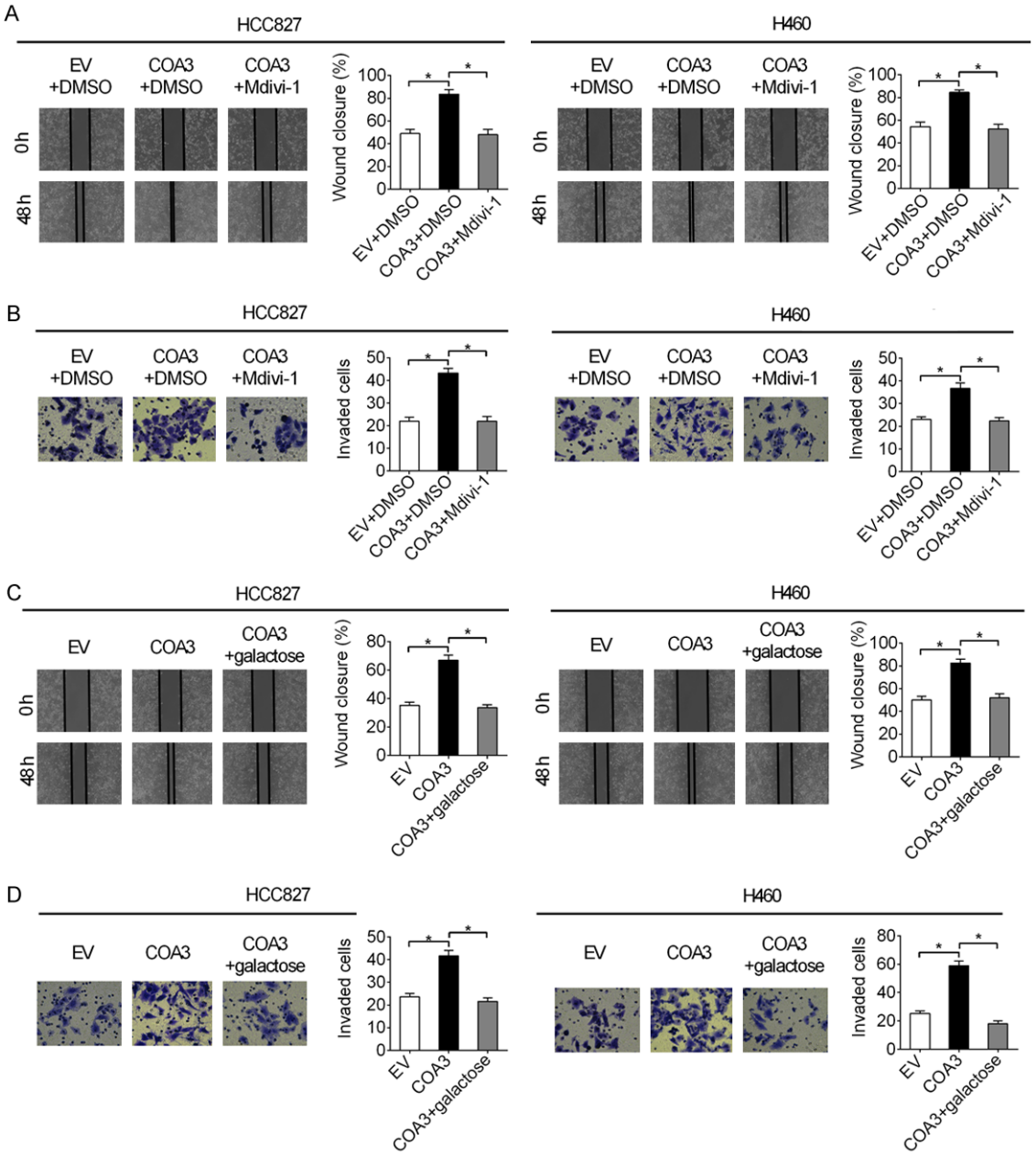

Figure 8. COA3 promotes NSCLC metastasis mainly through enhancing mitochondrial fragmentation-induced aerobic glycolysis. (A and B) Cell migration (A) and invasion (B) were evaluated in COA3 overexpression NSCLC cells upon mitochondrial fragmentation inhibition Mdivi-1. (C and D) Cell migration (C) and invasion (D) were evaluated in COA3 overexpression NSCLC cells upon glycolysis suppression by galactose.

ties. Conversely, forced COA3 expression enhanced the motility and invasiveness of NSCLC cells. These findings suggest that COA3 plays a critical role in the metastasis of NSCLC. Consistently, it was also demonstrated in breast cancer that COA3 was closely associated with tumor metastasis [17]. Moreover, we found that COA3 induced epithelial-mesenchymal transition (EMT) of NSCLC cells, suggesting that COA3 may promote NSCLC metastasis through activating EMT.

MicroRNAs (miRNAs) have been well-known as important post-transcriptional regulators of gene expression [18]. To determine whether the upregulation of COA3 is a consequence

microRNA dysregulation in NSCLC cells, we screened potential miRNAs targeting COA3 through bioinformatics analysis combined with experimental validation, and found that decreased miR-338-3p level contributed to COA3 upregulation in NSCLC cells. Previously, miR-338-3p has been reported to be downregulated in several types of cancers [19-21], including NSCLC [22]. In addition, it has also been demonstrated that miR-338-3p suppressed NSCLC growth and metastasis by regulating different targets [23, 24]. In line with this, we also demonstrated that decreased miR-338-3p contributed to COA3 upregulation and thus tumor metastasis in NSCLC. As gene expression regulation can occur at various levels, we cannot exclude the contribution of other factors in COA3 upregulation in NSCLC.

Mitochondrial are dynamic organelles participate in various biological processes, and their morphology are constantly regulated by dynamic balance of fusion and fission [25]. It has been demonstrated that COA3 promotes mitochondrial fragmentation by facilitating mitochondrial recruitment of DRP1 in HeLa cells [13]. Similarly, we also found in NSCLC cells that COA3 induced mitochondrial fragmentation by promoting mitochondrial recruitment of DRP1 via phosphorylating at Ser616. It has been well established that mitochondrial dysfunction is a main source of increased reactive oxygen species (ROS) production [26], which activates a series of protein phosphorylation-related signaling pathways, such as ERK and AKT kinase pathways [27]. Accordingly, we hypothesized that COA3 may promote the phosphorylation of DRP1 in NSCLC cells by activating ROS-related kinase pathways, which warrant further investigations. Previous studies have revealed that mitochondrial dynamic dysregulation played important roles in the progression of various human diseases, including cancer [28]. In NSCLC, mitochondria were reported to be significantly fragmented, which promoted the survival of NSCLC cells [29, 30]. Consistently, we also demonstrated that increased mitochondrial fragmentation contributed to COA3-promoted NSCLC metastasis, further supporting the crucial roles of increased mitochondrial fragmentation in cancer progression.

Reprogramming of glucose metabolism is a hallmark of cancer, but the molecular mechanisms remain to be identified. [31]. Over the past decade, studies have mainly focused on the roles of dysregulated oncogenes or tumor suppressors in increased aerobic glycolysis, the contribution of mitochondria dysfunction has received less attention [32]. Here, we discovered that COA3 upregulation was closely linked to increased aerobic glycolysis by inducing mitochondrial fragmentation in NSCLC cells. In line with our findings in NSCLC, it has also been reported that COA3 played a role in the promotion of a Warburg-like metabolic phenotype in breast cancer cells [17]. Moreover, we further found that mitochondrial fragmentation-promoted aerobic glycolysis is required for the promoting effect of COA3 in NSCLC metastasis. These findings collectively suggest that mitochondrial dynamic dysfunction plays crucial roles in metabolism reprogramming and disease progression in human cancers. Given that disruption of cytochrome c oxidase could also induce aerobic glycolysis through induction of Ca^{2+}-mediated retrograde signaling [33], we cannot exclude the possibility that other factors may also contribute to COA3-promoted aerobic glycolysis in NSCLC cells, which still needs further investigation.

In conclusion, we provide both clinical and mechanistic evidence that COA3 functions as an oncogene by inducing mitochondria fragmentation-mediated aerobic glycolysis in NSCLC cells, suggesting that COA3 could serve as a potential target for NSCLC treatment.

Acknowledgements

This study was supported by grants from Shaanxi Key R&D Program (2018ZDCXL-SF-02-03-02) and the National Natural Science Foundation of China (81970076).

Disclosure of conflict of interest

None.

Address correspondence to: Dr. Faguang Jin, Department of Respiratory and Critical Care Medicine, Tangdu Hospital, The Air Force Medical University, 1 Xinsi Road, Xi'an 710038, Shaanxi Province, China. Tel: +86-02984777425; E-mail: jinfag@fmmu.edu.cn

References

[1] Mak LY, Cruz-Ramón V, Chinchilla-López P, Torres HA, LoConte NK, Rice JP, Foxhall LE, Sturgis EM, Merrill JK, Bailey HH, Méndez-Sánchez N, Yuen MF and Hwang JP. Global epidemiology, prevention, and management of hepatocellular carcinoma. Am Soc Clin Oncol Educ Book 2018; 38: 262-279.

[2] Forner A, Reig M and Bruix J. Hepatocellular carcinoma. Lancet 2018; 391: 1301-1314.

[3] Au JS and Frenette CT. Management of hepatocellular carcinoma: current status and future directions. Gut Liver 2015; 9: 437-448.

[4] Annesley SJ and Fisher PR. Mitochondria in Health and Disease. Cells 2019; 8: 680.

[5] Tilokani L, Nagashima S, Paupe V and Prudent J. Mitochondrial dynamics: overview of molecular mechanisms. Essays Biochem 2018; 62: 341-360.

[6] Chan DC. Mitochondrial dynamics and its involvement in disease. Annu Rev Pathol 2020; 15: 235-259.

[7] Wanet A, Arnould T, Najimi M and Renard P. Connecting mitochondria, metabolism, and stem cell fate. Stem Cells Dev 2015; 24: 1957-1971.

[8] Clemente P, Peralta S, Cruz-Bermudez A, Echevarria L, Fontanesi F, Barrientos A, Fernandez-Moreno MA and Garesse R. hCOA3 stabilizes cytochrome c oxidase 1 (COX1) and promotes cytochrome c oxidase assembly in human mitochondria. J Biol Chem 2013; 288: 8321-8331.

[9] Mick DU, Dennerlein S, Wiese H, Reinhold R, Pacheu-Grau D, Lorenzi I, Sasarman F, Weraarpachai W, Shoubridge EA, Warscheid B and Rehling P. MITRAC links mitochondrial protein translocation to respiratory-chain assembly and translational regulation. Cell 2012; 151: 1528-1541.

[10] Chandrashekar DS, Bashel B, Balasubramanya SAH, Creighton CJ, Ponce-Rodriguez I, Chakravarthi B and Varambally S. UALCAN: a portal for facilitating tumor subgroup gene expression and survival analyses. Neoplasia 2017; 19: 649-658.

[11] Shirdel EA, Xie W, Mak TW and Jurisica I. NAViGaTing the micronome--using multiple microRNA prediction databases to identify signalling pathway-associated microRNAs. PLoS One 2011; 6: e17429.

[12] Rodrigues T and Ferraz LS. Therapeutic potential of targeting mitochondrial dynamics in cancer. Biochem Pharmacol 2020; 182: 114282.

[13] Ban-Ishihara R, Tomohiro-Takamiya S, Tani M, Baudier J, Ishihara N and Kuge O. COX assembly factor ccdc56 regulates mitochondrial morphology by affecting mitochondrial recruitment of Drp1. FEBS Lett 2015; 589: 3126-3132.

[14] Serasinghe MN and Chipuk JE. Mitochondrial fission in human diseases. Handb Exp Pharmacol 2017; 240: 159-188.

[15] Lee M and Yoon JH. Metabolic interplay between glycolysis and mitochondrial oxidation: The reverse Warburg effect and its therapeutic implication. World J Biol Chem 2015; 6: 148-161.

[16] Lu J. The Warburg metabolism fuels tumor metastasis. Cancer Metastasis Rev 2019; 38: 157-164.

[17] Meng F, Wu L, Dong L, Mitchell AV, James Block C, Liu J, Zhang H, Lu Q, Song WM, Zhang B, Chen W, Hu J, Wang J, Yang Q, Huttemann M and Wu G. EGFL9 promotes breast cancer metastasis by inducing cMET activation and metabolic reprogramming. Nat Commun 2019; 10: 5033.

[18] Vishnoi A and Rani S. MiRNA biogenesis and regulation of diseases: an overview. Methods Mol Biol 2017; 1509: 1-10.

[19] Zhang R, Shi H, Ren F, Feng W, Cao Y, Li G, Liu Z, Ji P and Zhang M. MicroRNA-338-3p suppresses ovarian cancer cells growth and metastasis: implication of Wnt/catenin beta and MEK/ERK signaling pathways. J Exp Clin Cancer Res 2019; 38: 494.

[20] Ji D, Hu G, Zhang X, Yu T and Yang J. Long noncoding RNA DSCAM-AS1 accelerates the progression of hepatocellular carcinoma via sponging miR-338-3p. Am J Transl Res 2019; 11: 4290-4302.

[21] Lu H, Zhang Q, Sun Y, Wu D and Liu L. LINC00689 induces gastric cancer progression via modulating the miR-338-3p/HOXA3 axis. J Gene Med 2020; 22: e3275.

[22] Sun J, Feng X, Gao S and Xiao Z. microRNA-338-3p functions as a tumor suppressor in human nonsmallcell lung carcinoma and targets Ras-related protein 14. Mol Med Rep 2015; 11: 1400-1406.

[23] Li Y, Chen P, Zu L, Liu B, Wang M and Zhou Q. MicroRNA-338-3p suppresses metastasis of lung cancer cells by targeting the EMT regulator Sox4. Am J Cancer Res 2016; 6: 127-140.

[24] Zhang P, Shao G, Lin X, Liu Y and Yang Z. MiR-338-3p inhibits the growth and invasion of non-small cell lung cancer cells by targeting IRS2. Am J Cancer Res 2017; 7: 53-63.

[25] Fenton AR, Jongens TA and Holzbaur ELF. Mitochondrial dynamics: shaping and remodeling an organelle network. Curr Opin Cell Biol 2021; 68: 28-36.

[26] Venditti P, Di Stefano L and Di Meo S. Mitochondrial metabolism of reactive oxygen species. Mitochondrion 2013; 13: 71-82.

[27] Moloney JN and Cotter TG. ROS signalling in the biology of cancer. Semin Cell Dev Biol 2018; 80: 50-64.
[28] Li L, Qi R, Zhang L, Yu Y, Hou J, Gu Y, Song D and Wang X. Potential biomarkers and targets of mitochondrial dynamics. Clin Transl Med 2021; 11: e529.
[29] Rehman J, Zhang HJ, Toth PT, Zhang Y, Marsboom G, Hong Z, Salgia R, Husain AN, Wietholt C and Archer SL. Inhibition of mitochondrial fission prevents cell cycle progression in lung cancer. FASEB J 2012; 26: 2175-2186.
[30] Seo JH, Chae YC, Kossenkov AV, Lee YG, Tang HY, Agarwal E, Gabrilovich DI, Languino LR, Speicher DW, Shastrula PK, Storaci AM, Ferrero S, Gaudioso G, Caroli M, Tosi D, Giroda M, Vaira V, Rebecca VW, Herlyn M, Xiao M, Fingerman D, Martorella A, Skordalakes E and Altieri DC. MFF regulation of mitochondrial cell death is a therapeutic target in cancer. Cancer Res 2019; 79: 6215-6226.
[31] Schwartz L, Supuran CT and Alfarouk KO. The Warburg effect and the hallmarks of cancer. Anticancer Agents Med Chem 2017; 17: 164-170.
[32] Park JH, Pyun WY and Park HW. Cancer metabolism: phenotype, signaling and therapeutic targets. Cells 2020; 9: 2308.
[33] Srinivasan S, Guha M, Dong DW, Whelan KA, Ruthel G, Uchikado Y, Natsugoe S, Nakagawa H and Avadhani NG. Disruption of cytochrome C oxidase function induces the Warburg effect and metabolic reprogramming. Oncogene 2016; 35: 1585-1595.

Table S1. Sequence of primers for qRT-PCR analysis

COA3	forward primer	ACACCCGAGCAACTGCATT
	reverse primer	GAAACGCTCCTGGGAAATCG
E-cadherin	forward primer	GGCCCAGGAGCTGACAAAC
	reverse primer	GTGGATGGCAAAGTGGTGTC
ZO-1	forward primer	CAACATACAGTGACGCTTCACA
	reverse primer	CACTATTGACGTTTCCCCACTC
N-cadherin	forward primer	CACTGCTCAGGACCCAGAT
	reverse primer	TAAGCCGAGTGATGGTCC
Vimentin	forward primer	TCGTTTCGAGGTTTTCGCGTTAGAGAC
	reverse primer	CGACTAAAACTC GACCGACTCGCGA
MFN1	forward primer	TGGCTAAGAAGGCGATTACTGC
	reverse primer	TCTCCGAGATAGCACCTCACC
MFN2	forward primer	CTCTCGATGCAACTCTATCGTC
	reverse primer	TCCTGTACGTGTCTTCAAGGAA
OPA1	forward primer	TGTGAGGTCTGCCAGTCTTTA
	reverse primer	TGTCCTTAATTGGGGTCGTTG
DRP1	forward primer	GGAGACTCATCTTTGGTGAAGAG
	reverse primer	AAGGAGCCAGTCAAATTATTGC
FIS1	forward primer	GTCCAAGAGCACGCAGTTTG
	reverse primer	ATGCCTTTACGGATGTCATCATT
MFF	forward primer	ACTGAAGGCATTAGTCAGCGA
	reverse primer	TCCTGCTACAACAATCCTCTCC
β-actin	forward primer	GGCTGTATTCCCCTCCATCG
	reverse primer	CCAGTTGGTAACAATGCCATGT

Table S2. Association between expressions of COA3 and the clinicopathological features of NSCLC patients

Clinicopathological features	No. of cases (%)	COA3 expression		*P* value
		Low	High	
All	281 (100%)	140	141	
Age				
<60	109 (%)	49	60	0.221
≥60	172 (%)	91	81	
Gender				
Female	83 (%)	44	39	0.515
Male	198 (%)	96	102	
Tumor size (cm)				
<3	74 (%)	30	44	0.078
≥3	207 (%)	110	97	
Stage				
I+II	176 (%)	82	94	0.176
III+IV	105 (%)	58	47	
Lymph node metastasis				
No	131 (%)	56	75	0.031
Yes	150 (%)	84	66	

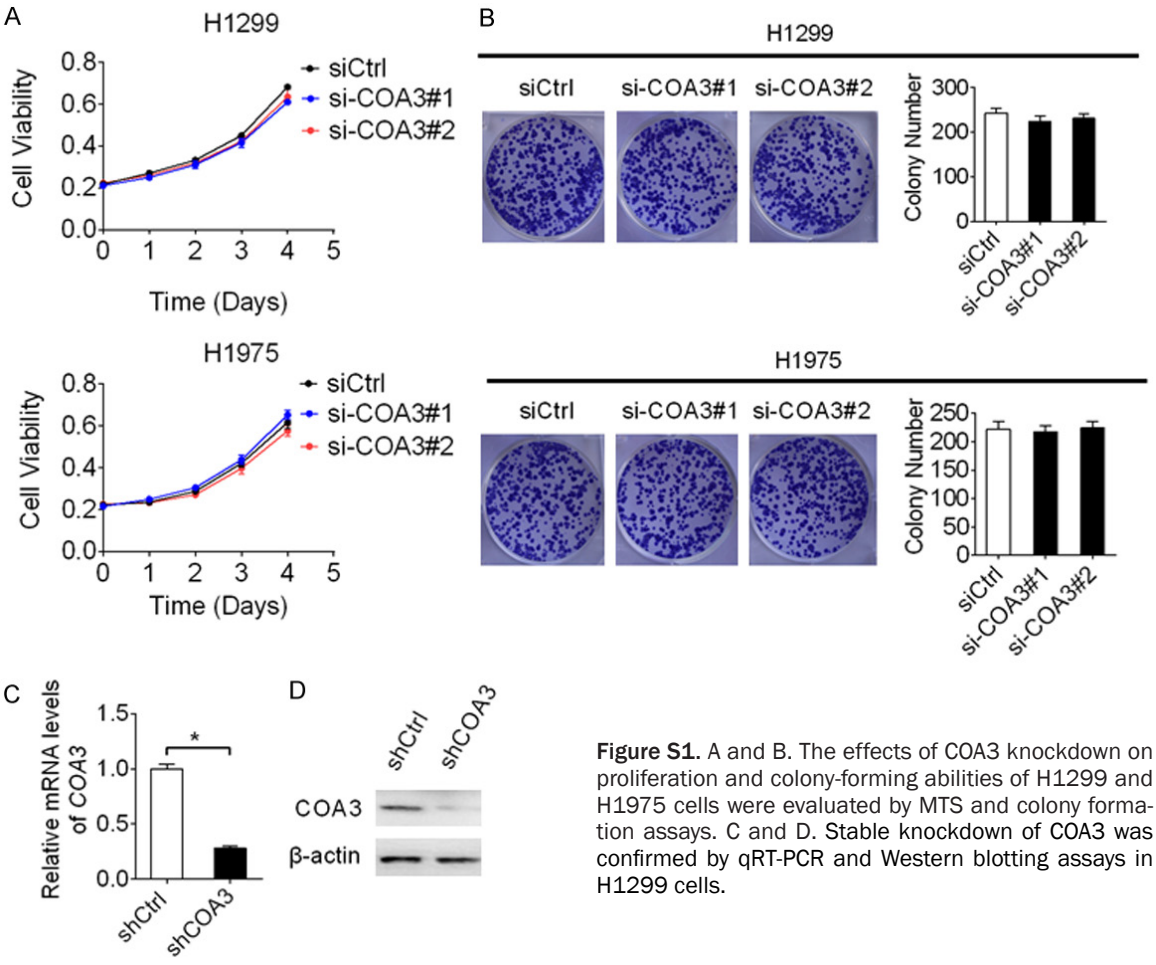

Figure S1. A and B. The effects of COA3 knockdown on proliferation and colony-forming abilities of H1299 and H1975 cells were evaluated by MTS and colony formation assays. C and D. Stable knockdown of COA3 was confirmed by qRT-PCR and Western blotting assays in H1299 cells.

A

Gene symbol	microRNA	Integrated Score	Number of Sources	Score class
COA3	miR-371a-5p	0.685	13	very high
COA3	miR-24-3p	0.642	17	very high
COA3	miR-338-3p	0.636	11	high
COA3	miR-635	0.595	11	high
COA3	miR-22-3p	0.391	12	high

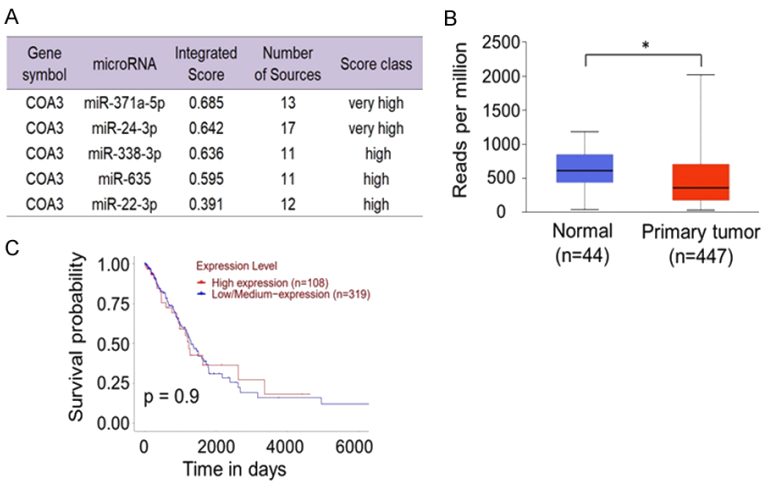

Figure S2. (A) Top five predicted miRNAs targeting COA3 by using the microRNA Data Integration Portal (mirDIP)-based target prediction [1]. (B and C) Bioinformatics analysis for the expression (B) and prognostic significance (C) of miR-338 was conducted in NSCLC TCGA data using the online web portal UALCAN.

Reference

[1] Tokar T, Pastrello C, Rossos AEM, Abovsky M, Hauschild AC, Tsay M, Lu R and Jurisica I. mirDIP 4.1-integrative database of human microRNA target predictions. Nucleic Acids Res 2018; 46: D360-D370.